

Helsinki University of Technology Applied Electronics Laboratory

Series E: Electronic Publications E1

Teknillisen korkeakoulun sovelletun elektroniikan laboratorio; sarja E: Elektronisia julkaisuja E1
Espoo 2002

METHODS FOR INTERVENTIONAL MAGNETIC RESONANCE IMAGING

Erkki Vahala

Dissertation for the degree of Doctor of Science in Technology to be presented with due permission of the Department of Electrical and Communications Engineering, for public examination and debate in Auditorium S3 at Helsinki University of Technology (Espoo, Finland) on the 18th of December, 2002, at 12 noon.

Helsinki University of Technology
Department of Electrical and Communications Engineering
Applied Electronics Laboratory

Teknillinen korkeakoulu
Sähkö- ja tietoliikennetekniikan osasto
Sovelletun elektroniikan laboratorio

Distribution:
Helsinki University of Technology
Applied Electronics Laboratory
P.O. Box 3000
FIN-02015 HUT, Finland

Copyright © 2002 Erkki Vahala

ISBN 951-22-6132-4
ISSN 1459-1111

Contents

Abstract	iv
Acknowledgements	v
List of Publications	vi
Abbreviations	vii
1 Introduction	1
1.1 Purpose of the Study	2
1.2 Organization.....	2
1.3 MR Theory	3
1.3.1 Nuclear Magnetic Resonance	3
1.3.2 Magnetic Resonance Imaging.....	3
1.3.2.1 Imaging Sequences	5
1.3.3 Electron Spin Resonance (ESR).....	7
1.3.4 Overhauser Effect.....	7
1.4 Instrument Tracking.....	8
1.4.1 Passive Detection.....	8
1.4.2 Auxiliary Tracking Devices	9
1.4.2.1 Optical Navigation.....	9
1.5 MR Thermometry for Thermal Treatment of Tumours.....	10
2 Methods and Results	13
2.1 Overhauser Enhanced Instrument Localization (I)	13
2.2 ESR Probe for Instrument Tracking (II).....	14
2.3 Optical Tracking (III–V)	15
2.3.1 System Description.....	15
2.3.1.1 Hardware.....	15
2.3.1.2 User Interface	16
2.3.1.2.1 Calibration.....	16
2.3.1.2.2 Intraoperative Use	17
2.3.2 Clinical Applications.....	19
2.3.2.1 Nerve Root Infiltration.....	19
2.3.2.2 Bone Biopsies.....	19
2.3.2.3 Patient Tracking	19
2.4 MR Thermometry of Liver Tissue (VI).....	20
3 Discussion	22
4 Conclusions	25
5 References	26
6 Articles	32

Abstract

This thesis has as its central aim to demonstrate, develop, discuss and promote new methods and technology for improving interventional low field magnetic resonance imaging. The work addresses problems related to accurate localization of minimally invasive surgical tools by describing novel devices and improvements to prior art techniques, such as optical tracking. In addition to instrument guidance, ablative treatment of liver tumours is discussed in connection with low field temperature measurement and the work describes suitable sequences for qualitative temperature imaging.

For instrument localization, a method utilising ex vivo Overhauser enhancement of a catheter like structure was demonstrated. An enhancement factor of 10 was achieved, proving that a substantial signal gain is possible through the use of ex vivo-enhanced liquid. Similarly, a method for biopsy needle tip tracking was developed; where the position of the tip was tracked with a signal from a miniaturized electron spin resonance sample and gradient pulses. At an update rate of 10 samples per second, the accuracy was measured to be better than ± 2 mm within a homogeneous sphere of 300 mm.

Optical tracking methods concentrated on new indications of use for the developed optical tracking system and associated software: The system was applied to guide the needle 35 times into first sacral root foramina, with a success rate of 97%. It was also used in five bone biopsies, all of which were performed successfully, the samples allowed for a pathologic diagnosis, and the percutaneous procedures could be performed in less than 40 minutes. A new patient tracker device was developed for staged neurosurgical procedures and demonstrated with two patient cases.

In the temperature measurement study, spin echo, gradient echo and completely balanced steady-state free precession sequences were optimized for maximal temperature sensitivity and the optimized sequences compared. The steady-state sequence seemed the most promising for the prediction of ablated volume in liver.

Keywords: Interventional MRI, Overhauser, Electron Spin Resonance, Optical Tracking, Thermal Ablation.

Acknowledgements

This work was carried out at the research and development department of Philips Medical Systems MR Technologies Finland, Ltd. The company has provided an excellent working environment with its friendly and supportive staff. Especially, it has been a great privilege to work under Dr. Gösta Ehnholm, whom I must thank for his good-humoured and knowledgeable guidance throughout the project. My thanks also go to my colleagues, Drs. Mika Ylihautala and Teuvo Vaara, in their advisory roles, and for proof-reading. Thank you for your shrewd comments, corrections and suggestions—working with such great minds leaves one humbled. The general manager of the company, Dr. Teppo Jyrkkiö, has provided financial and moral support, without which this thesis would not exist.

I am grateful to Professor Sepponen for initially arranging me the opportunity to work under my present employer and, later on, for the support towards my thesis. I am also grateful to Drs. Markku Komu and Antti Lamminen, the External Examiners of this thesis, for their constructive critique and suggestions for improvements.

It is my pleasure to thank (in no particular order) Professor Carl-Gustaf Standertskjöld-Nordenstam and his staff at Helsinki University of Central Hospital; Professor Hervé Saint-Jalmes at Laboratoire de Résonance Magnétique Nucléaire Méthodologique et Instrumentation en Biophysique; Professor John Koivukangas, Docent Osmo Tervonen, and their staffs at University Hospital of Oulu; Professor Ian Young, FRS, at Robert Steiner MRI Unit, Hammersmith Hospital, London; Dr. Klaes Golman and his staff at Amersham Health Ab; and Dr. Riitta Parkkola and her staff at University of Turku. Collaboration with these individuals and organizations has been a very pleasant experience.

The following individuals and their contributions are also acknowledged with deepest gratitude: Dr. Delphine Germain, Dr. Ib Leunbach, Dr. Jarmo Ruohonen, Dr. Thomas Andreae, Yrjö Markkanen, Pasi Väisänen, Nina Etelä, Dr. Mikko Uusitalo, Lasse Jyrkinen and Dr. Risto Ojala.

I am indebted to Elsevier Science and John Wiley & Sons for leave to make use of their published material here.

Vantaa
November 2002

E.V.

List of Publications

This thesis consists of an introductory part and the six publications listed below. In the introductory part, the articles are referred to with their roman numerals.

- I Vahala E, Ylihautala M, Ehnholm G, Etelä N, Young I, Golman K, Leunbach I. A Study of the Use of Overhauser Enhancement to Assist with Needle and Catheter Placement during Interventional MRI. *Journal of Magnetic Resonance* 157:298–303 (2002). DOI 10.1006/jmre.2002.2595.
- II Ehnholm G, Vahala E, Kinnunen J, Nieminen J, Standertskjöld-Nordenstam CGM, Uusitalo M. Electron Spin Resonance (ESR) Probe for Interventional MRI Instrument Localization. *Journal of Magnetic Resonance Imaging* 10:216–219 (1999).
- III Ojala R, Vahala E, Karppinen J, Klemola R, Blanco Sequeiros R, Vaara T, Tervonen O. Nerve Root Infiltration of the First Sacral Root With MRI Guidance. *Journal of Magnetic Resonance Imaging* 12:556–561 (2000).
- IV Ojala R, Blanco Sequeiros R, Klemola R, Vahala E, Jyrkinen L, Tervonen O. MR-Guided Bone Biopsy: Preliminary Report of a New Guiding Method. *Journal of Magnetic Resonance Imaging* 15:82–86 (2002).
- V Vahala E, Ylihautala M, Tuominen J, Schiffbauer H, Katisko J, Yrjänä S, Vaara T, Ehnholm G, Koivukangas J. Registration in Interventional Procedures With Optical Navigator. *Journal of Magnetic Resonance Imaging* 13:93–98 (2001).
- VI Germain D, Vahala E, Ehnholm G, Vaara T, Ylihautala M, Savart M, Laurent A, Tantt J, Saint-Jalmes H. MR Temperature Measurement in Liver Tissue at 0.23 T With a Steady-State Free Precession Sequence. *Magnetic Resonance in Medicine* 47:940–947 (2002). DOI 10.1002/mrm.10147.

The author has partaken in the experiments described in publications I and VI, with the sole responsibility of the experiments in II and writing of the articles in all save IV. The author has developed navigational devices and software for the methods described in I–V. In all cases, the author has had the role of principal physicist.

Abbreviations

MRI	Magnetic Resonance Imaging
CT	Computed Tomography
IMRI	Interventional Magnetic Resonance Imaging
FID	Free Induction Decay
SNR	Signal-to-Noise Ratio
TR	Repetition Time
SSFP	Steady-State Free Precession
ESR	Electron Spin Resonance
FT-ESR	Fourier Transformed Electron Spin Resonance
DNP	Dynamic Nuclear Polarization
LITT	Laser-Induced Thermotherapy
FSE	Fast Spin Echo
TE	Echo Time
PVC	Polyvinylchloride

1 Introduction

Advancement in the field of Magnetic Resonance Imaging (MRI) has been considerable during the last two decades. What was originally perceived as a method for diagnostic study of cancerous tissue [1] is now a multidisciplinary tool; its applicability varying from the study of the functionality of the brain [2] to the quasi real time guidance of surgical tools [3].

The main reasons for the wide-spread adaptation of MRI lie in its superior soft-tissue contrast as compared to competing modalities, such as ultrasound or computed tomography (CT); versatility of the underlying physical phenomena; and the lack of deleterious effects on patients and operators alike [4, 5]. These advantages, together with the constantly improving performance of MRI equipment and the introduction of open-configuration magnets with easy patient access, have recently made MRI an eminent choice for conducting interventional procedures—that is, the procedures where an imaging modality is used to facilitate invasive, typically percutaneous operations.

To utilize the potential of interventional MRI, methods and paraphernalia, compatible with the demanding environment an Magnetic Resonance (MR) scanner presents, are needed [6, 7]. A rather obvious interventional method for an imaging modality is the guidance of tools when direct visual contact to a target is lost or not applicable. For instance, the placement of biopsy needles or catheters, or localizing contrast-enhancing tissue during a craniotomy benefits from the additional information provided by MR images. Navigational devices for augmenting the guidance, such as optical tracking systems or specialized magnet dependent instrument trackers, have been described in literature.

In addition to guided imaging, MRI can also be used for extracting localized temporal information about the temperature in tissue. This unique feature opens new vistas for monitoring minimally invasive therapeutic operations where local tissue necrosis is intentionally induced by heating [8, 9].

However, there are performance-limiting technical problems with interventional procedures on open configuration magnets. The mechanical structure of such magnets does not allow as strong magnetic fields to be used as with solenoid magnets, which results in relatively low signal to noise ratio. This in turn hampers many of the operations, as the needed near real-time imaging times are limited by noise. For example, the detection of Gadolinium filled catheter requires high resolution, as the lumen can be only 1 mm in diameter, effectively ruling out fast

image acquisition. One way to circumvent the real-time requirements for the imager is to use real-time tracking systems with rigid instruments. But one of the disadvantages in using external trackers is the need for complex and time-consuming registration and calibration routines. In addition, the rigidity of instruments, such as biopsy needles, cannot always be guaranteed and the uncertainty in tip position can ruin otherwise good accuracy of the tracking system.

1.1 Purpose of the Study

This thesis concerns the methodology in the nascent field of interventional MRI. The aim has been to develop novel methods and technology for low field scanners that would ultimately result in safer, faster and more accurate interventional procedures than presently available.

1. More specifically, novel localization and guiding methods are described that attempt to tackle the problems associated with the limited accuracy of passive instrument tracking and optical navigator systems:
 - a) One goal has been to demonstrate substantial enhancement in the signal to noise ratio in liquid filled structures, such as catheters, which would eventually allow for faster and more accurate localization of the said structures.
 - b) Also means for measuring the tip position of a thin semirigid needle have been sought to combat the needle bending, the aim being a demonstration of tip tracking in vitro.
2. Improvements to optical navigation were to be devised—via the integration of a navigator system with an MR scanner and development of new registration and calibration procedures—and tested with both intraoperative use and neuronavigation in clinical settings. The goal was to demonstrate in practice an ergonomic, accurate, fast and versatile system for a range of interventional procedures.
3. Finally, the applicability of a low field scanner to the temperature monitoring of liver tissue was examined and improvements to signal to noise in temperature images sought through simulations and measurements on different sequence types and sequence parameters.

1.2 Organization

The text has been arranged into several sections, of which the first section (chapters 1.3–1.5) introduces the theory, terminology and relevant concepts that are used in the subsequent chapters. The second section outlines the actual methods and results (chapter 2), the third is a discussion of the results (chapters 3–4) and the fourth lists the publications arising from the work (chapter 6).

1.3 MR Theory

The physical principles of magnetic resonance imaging have a profound effect on the methodology and devices available for interventional MRI (IMRI). Not only does the characteristic signal behaviour affect the procedures but also the interaction between magnet and auxiliary equipment is a major factor. Therefore, it is necessary to understand the basic physics governing an imaging event in order to be able to better appreciate the reasons behind design choices in MR compatible equipment.

1.3.1 Nuclear Magnetic Resonance

A spin, or spin angular momentum, is a discretely quantized property that is associated with quantum mechanical behaviour of nuclear particles. The magnetic dipole moment of a particle is directly proportional to its spin, and placing the particle into an external magnetic field, denoted by the magnetic flux density \mathbf{B}_0 , results in Zeeman interaction and a Hamiltonian operator, H , of the form $H = -\gamma\hbar\mathbf{B}_0 I_z$ (\mathbf{B}_0 chosen to be along an arbitrary z -axis). The constant γ is the gyromagnetic ratio characteristic for the type of the particle; \hbar Planck's constant h , $\approx 6.63 \times 10^{-34}$ Js, divided by 2π ; and I_z the operator for the angular momentum along the z -axis. Because the interaction energy is quantized, only integer difference steps between eigenvalues of I_z are allowed, and gaps between energy levels are of constant value [10]. Using the definition for a quantum of energy, $\varepsilon = hf$, where f is the characteristic frequency, a gap corresponds to $f_0 = \gamma\mathbf{B}_0$ [11], where γ is the gyromagnetic ratio divided by 2π . The frequency f_0 is known as the Larmor frequency, and irradiation with an electromagnetic field at that frequency can induce changes in the state the particle is in.

In the simplest non-trivial spin system, the eigenvalues are $+1/2$ and $-1/2$. Most notably, protons form such a system. The system has two energy levels available and the population of the levels in thermal equilibrium can be solved using Maxwell–Boltzmann distribution function. For example, $a_{+1/2}$, the fraction of particles in the state corresponding to the eigenvalue of $+1/2$, is:

$$a_{+1/2} = \frac{\exp\left(\frac{+1/2 \cdot \gamma\hbar\mathbf{B}_0}{k_B T}\right)}{\exp\left(\frac{+1/2 \cdot \gamma\hbar\mathbf{B}_0}{k_B T}\right) + \exp\left(\frac{-1/2 \cdot \gamma\hbar\mathbf{B}_0}{k_B T}\right)} \quad [1]$$

Where k_B is the Boltzmann's constant, $\approx 1.38 \times 10^{-23}$ JK⁻¹, and T the temperature. It should be noted that at room temperature, a proton system has a very slight (of order 10^{-6} , when \mathbf{B}_0 equals 0.23 T) imbalance in favour of the lower energy state. In semi-classical picture, the difference creates a small but measurable net magnetization, \mathbf{M} , for the system.

1.3.2 Magnetic Resonance Imaging

In MRI, the prevalent use of large, nearly independent proton ensembles as a signal source makes it possible to use classical mechanics to describe proton behaviour under the effect of

\mathbf{B}_0 and irradiation field \mathbf{B}_1 . The rate of change of magnetization is then governed by Bloch equations, presented here in matrix form [12]:

$$\frac{d\mathbf{M}}{dt} = \gamma\mathbf{M} \times \mathbf{B} - \begin{bmatrix} T_2^{-1} & 0 & 0 \\ 0 & T_2^{-1} & 0 \\ 0 & 0 & T_1^{-1} \end{bmatrix} (\mathbf{M} - \mathbf{M}_0) \quad [2]$$

Here \mathbf{B} denotes the combination of magnetic field components acting upon protons—conventionally, with \mathbf{B}_1 orthogonal to \mathbf{B}_0 : $\mathbf{B} = i\mathbf{B}_{1x} + j\mathbf{B}_{1y} + k\mathbf{B}_0$. T_1 is the longitudinal relaxation time constant effecting the restoration of magnetization along the longitudinal magnetic field, \mathbf{B}_0 . T_2 is the transverse relaxation time constant describing the restoration of thermal equilibrium among the spins. \mathbf{M}_0 is the initial equilibrium value for magnetization.

With a suitable strong irradiation pulse of duration Δt ($\Delta t \ll T_2$), it is possible to temporarily tilt the magnetization vector to x–y plane, where it keeps rotating at its Larmor frequency. The rotation can be measured by detecting the induced electromotive force in a receiver coil.

Because of the relaxation effects, the signal diminishes with time, producing a characteristic envelope on the oscillating voltage. This is called free induction decay (FID). In addition to the net magnetization dependence (cf.), the induced voltage also depends directly on \mathbf{B}_0 as a result of Faraday's law of electromagnetic induction and the definition of Larmor frequency. Therefore, strong \mathbf{B}_0 -fields, 0.2–3 T, are used in commercial systems to produce images with high enough signal-to-noise ratio (SNR) for clinical use.

Spatial magnetic field gradients can be used to encode the position information of a signal sourcing spin system into the received signal [13]. With well-controlled monotonous gradients in the volume of interest, it is possible to decode the positions of signal sources and reconstruct images from the spin system.

1.3.2.1 Imaging Sequences

There is a multitude of different position encoding schemes for producing MR images [10]. Temporal gradient, measurement read-out, and B_1 -pulse events can be used to characterize typical diagnostic encoding schemes into different categories, or sequence types. For example, a field echo sequence (see Figure 1) comprises cycles of consecutive slice selection, gradient encoding and gradient read-out events.

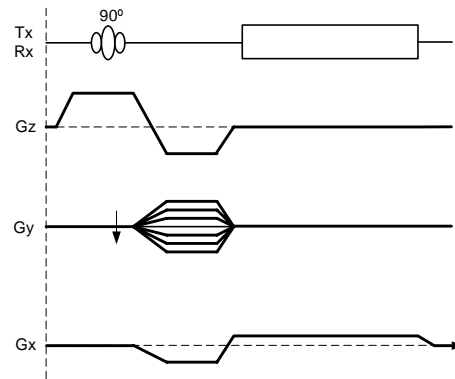


Figure 1. A single cycle from a field echo sequence. Tx/Rx line shows an irradiation pulse (ellipses) and a sampling window (rectangle). Gz denotes the slice selection gradient, Gy the ‘phase’ direction gradient and Gx the ‘frequency’ direction gradient.

In the slice selection events, a slice of the target volume is excited by allowing only a part of the target spins to be exposed to the magnetic field that matches the irradiation pulse frequency. In the encoding events, orthogonal ‘phase’ (Gy) and ‘frequency’ (Gx) gradients are momentarily turned on. In the read-out events, Gx is reversed to restore partly the coherence lost during the encoding events. The restoration produces a measurable signal echo, which is then sampled. Varying the strength of Gy and using Fourier transform reconstruction techniques, an image can be readily constructed from the measured samples—For an elegant illustration of the underlying encoding and decoding principles, see Ref. 14. A spin echo sequence (see Figure 2) is another simple imaging sequence, where the main difference, as compared to the field echo sequence, is the insertion of phase reversing irradiation pulse events after the encoding events. The phase reversal has the advantage of balancing out the static field inhomogeneities, but at the cost of a slightly longer repetition time (TR) of a cycle and a requirement for a well-calibrated irradiation pulse.

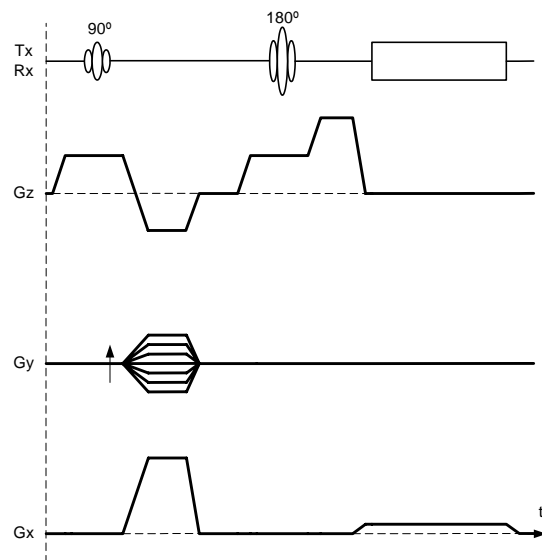


Figure 2. A single cycle from a spin echo sequence.

The structure of the third example, a completely balanced steady-state free precession (SSFP) sequence, is more convoluted than those of the above-mentioned basic sequences. It utilizes magnetization fulfilling the steady-state free precession condition that is generated by a train of event cycles. One such a cycle is depicted in Figure 3.

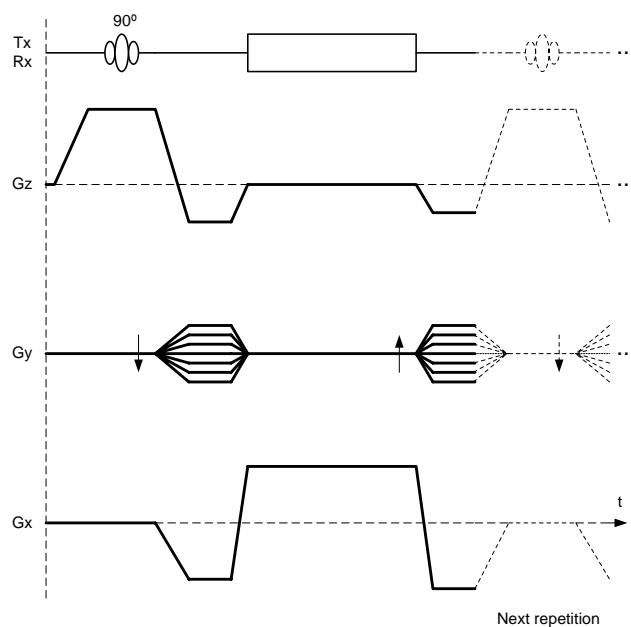


Figure 3. Timing diagram of a completely balanced steady-state free precession sequence.

Each cycle generates a SSFP FID, that is, an echo signal produced by the irradiation pulse at the beginning of the cycle. The gradient reversals at the end of the cycle refocus the FID: Transverse magnetization components that have phase shifted $2\pi n$ radians (where n is an integer value) with respect to the nominal Larmor frequency during the TR period regain the phase values they had at the beginning of the cycle. The phase-inversed irradiation pulse of the next cycle restores refocused transverse components along the longitudinal axis, boosting the longitudinal magnetization that is regenerated during the next cycle. Because all three gradient directions are used in refocusing, the sequence is known as ‘completely balanced’. In addition to the SSFP FID, also SSFP echoes, or ‘time-reversed echoes’, are produced as coherent magnetization is carried from one cycle to the next. In this particular case, the time-reversed echo coincides with the FID, so that the signals add up. It is obvious that in order to carry the magnetization from one cycle to another, the T_2 of the spin system should be longer than or comparable to the TR of the sequence. Because of the steady-state magnetization, TR can be made short while maintaining good SNR. The downside is the need for a very homogeneous main field, as the phase shift conditions must be met within the volume of interest to maximize the signal. [10, 15].

1.3.3 *Electron Spin Resonance (ESR)*

Some of the paramagnetic substances are suitable for electron spin resonance; That is, instead of proton spins, electron spins can be irradiated and irradiation effects detected directly from the signal emitted by electrons. In electron paramagnetic resonance spectroscopy, this is known as pulse Electron Spin Resonance (pulse ESR), or FT-ESR (Fourier Transformed ESR). Because of the high gyromagnetic ratio, ~ 658 times that of a proton, and short relaxation time constants in microseconds range in room temperatures, the direct detection of FID is difficult and requires sophisticated microwave electronics even on low-field magnets [16, 17]; Alternatively, the altered susceptibility can be used to observe resonance with specialized equipment [18, 19], bearing close resemblance to continuous-wave ESR [20]. Because of the high gyromagnetic ratio, the signal from a sample is very strong and the sample can be made minuscule while still maintaining an acceptable signal-to-noise ratio.

1.3.4 *Overhauser Effect*

The obtainable proton signal is directly dependent of the transverse net magnetization; therefore, one method to improve signal-to-noise ratio is to boost net magnetization from its equilibrium value (cf.). This is possible through dynamic nuclear polarization (DNP) of Overhauser type [21]. In DNP, certain favourable paramagnetic agents can temporarily enhance net magnetization by polarization transfer from pre-irradiated paramagnetic centres to protons. Overhauser enhancing large in vivo volumes is technically difficult because of the high gyromagnetic ratio of electrons: the skin depth effect limits the penetration of irradiation field at the ESR frequency and unconventional methods such as field-cycling are needed [22]. However, Overhauser enhanced signal can be used for detecting very small structures and markers using conventional MR imaging techniques [23, 24].

1.4 Instrument Tracking

The detection of interventional tools on MR images can be arranged either by passive means, where the induced artefacts on acquired images indicate the instrument position, or by utilising tools equipped with auxiliary tracking devices. The auxiliary devices can be independent tracking systems, such as mechanical wands [25, 26], sonic or optical localizers [27–29], or stereotaxic frames [30, 31, 32] that take preoperative MR images as input data, or more integrated systems that allow intraoperative use [33] and even rely on the scanner hardware to provide the position information [34–38].

1.4.1 *Passive Detection*

The advantages of passive detection lie in its simplicity and reliability—no extra hardware is needed for tracking. On the other hand, because the detection relies on image acquisition, real-time response is difficult to achieve, as is accurate image acquisition control: To minimize image acquisition time, the number of slices should be small. This means that those few slices must be optimally aligned to show only the instrument and pertinent parts of anatomy. The imaging planes need to be manually re-aligned to account for changes in instrument position, which is time consuming and error-prone. In addition, the susceptibility artefacts tend to be unreliable in appearance and exhibit dependencies on the relative direction of the instrument with the \mathbf{B}_0 field and imaging sequence parameters [39]. Conspicuity problems are especially severe on low field scanners, where SNR limits many of the operations. Typical uses of passive detection include the detection of surface treated titanium needles [39–41], doped catheters [42, 43] and MR-visible marker structures—such as fiducials [44], cylindrical pointers (TrackPointer™, MRI Devices Daum GmbH, Schwerin, Germany) or catheters [45] filled with contrast enhancing liquid. The first two of the aforementioned rely on the induced signal voids in the images and require manufacturing processes that produce well-controlled, field-dependent artefacts. Cf. Figure 4. Containers for MR-visible substances are generally limited for image registration and initial alignment of tools and imaging planes; they required large volumes to produce enough signal, which makes percutaneous operations difficult. Filled catheters find more use in high field systems, where the quasi real time imaging is made possible by the inherently high SNR.

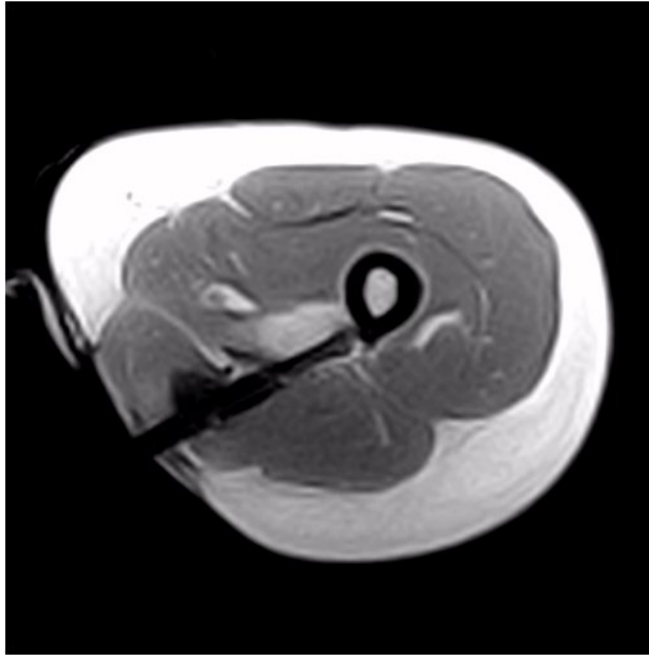


Figure 4. A T_1 -weighted image showing a needle artefact on a recurrent desmoid tumour of the leg.

1.4.2 Auxiliary Tracking Devices

Independent tracking devices have originally been developed in the 80's for CT, where the benefits of guidance without a scanner are obvious [46, 47]. The devices utilized mechanical arm, ultrasound, electromagnetic and optical tracking systems [6, 48, 49]. Because of the requirements for intraoperative MR compatibility, their adaptation to MR environment has meant extensive modifications to the hardware. In practice, this has resulted in widespread use of optical tracking systems, as the needed modifications have been the least drastic.

1.4.2.1 Optical Navigation

Optical navigation is based on the principle of optical triangulation, where either reflected (passive marker systems) or emitted (active marker systems) optical signals are recorded with rigidly fixed sensors. In the simplest case, the signal comes from a spot-like marker whose location in three dimensions can then be solved. With three or more markers attached to an instrument to be tracked, it is possible to calculate the position and rotation information of the instrument from the tracked positions of the markers. In medical use, the passive marker systems have advantage over active ones, as they can be made wireless and hence more ergonomic to use and less difficult to keep sterile. Such instrument trackers are depicted in Figure 5.

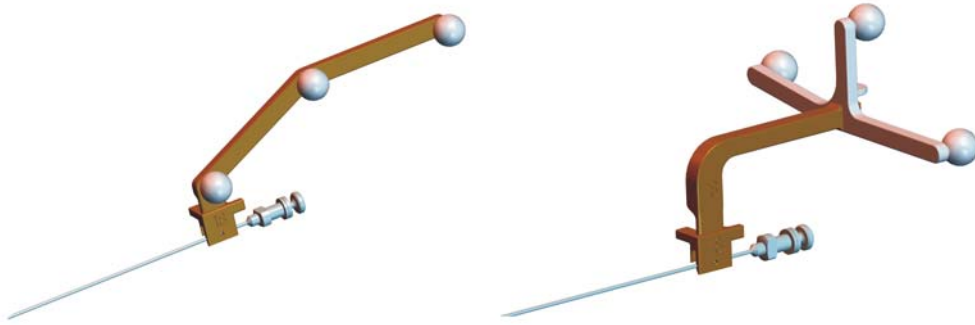


Figure 5. Needle trackers for 18 G semirigid needles. The bodies are made out of autoclavable plastic, and the single-use reflector spheres can be attached with a snap-on mechanism onto them. A needle goes into a groove on the tracker body and is fixed with a separate friction lock.

Because of the origins in CT, the first navigators to utilize MR were stand-alone units that displayed the instrument position on preoperative images to guide neurosurgical tools outside a scanner, much akin to neuronavigation with CT images [50]. The systems lacked interactive scanning capabilities, which meant that the brain shift, i.e. the swelling of brain tissue after the dura is opened, and tissue deformations during a procedure had adverse effects on the overall accuracy of the navigation [51], and resection completeness could not be easily ascertained. More integrated solutions were eventually developed; either by fixing the optical sensors to the scanner, as was done with the 0.5 T open-configuration magnet at Brigham and Women's Hospital in Boston [52, 53]; or by providing optical reference frames [54]. These allowed intraoperative imaging and introduced new indications for use as instrument guided quasi real time imaging became possible.

The registration of images with optical tracking system coordinates is typically done with fiducials: three or more fiducials are imaged, identified on the images, and pointed at with an optically tracked instrument that has been separately calibrated prior to registration [55, 56]. The formed coordinate pairs can then be used to calculate the transformation matrix [57]. With stand-alone systems, this procedure has to be repeated with every patient. The integrated tracking systems require calibration less often, and the periodic registration checks act as quality assurance for the system.

1.5 MR Thermometry for Thermal Treatment of Tumours

Rapid local temperature changes in tissue result in localized necrosis as the cells are either coagulated (hyperthermia) or frozen (hypothermia). This forms the basis for thermosensitive interstitial therapy, where a localized temperature change is generated inside a tumour so that the necrotic volume is limited to consist mainly of cancerous tissue, without excessive damage

to surrounding structures. The localized temperature change can also be utilized for other forms of therapy, such as local drug delivery with thermosensitive carriers [58]. Two commonly used cross-modal hyperthermic methods to induce localized tissue heating are Laser-Induced Thermotherapy (LITT) and radio frequency ablation [59]. In addition, microwave and focused ultrasound induced heating have been investigated for MR-guided procedures [60–62] and cryoablaters have been successfully demonstrated [63]. The detection of frozen tissue can also be arranged with other modalities, and thermosensitive contrast agents can be used for detecting threshold temperatures [64]—but MR appears to be particularly well suited for measuring gradual temperature changes in tissue [65].

LITT is particularly suited for MR-guided interstitial therapy, as the applicator consists of non-magnetic, non-conductive optical fibres. Also commercial radio frequency ablaters have been adapted for MR environment [66]. One of the promising application areas for the methods is palliative treatment of inoperable liver tumours [67]. In such a procedure, a small applicator is guided percutaneously into the tumour and a heat dose delivered. The requirements for the dose amount are contradictory: All of the cancerous tissue should be destroyed; meanwhile the destruction of healthy tissue or damage to sensitive areas around the tumour should be avoided. To find the optimal size and shape for the treated volume, means for monitoring the temperature distribution would be beneficial as the expanding thermal front is closely linked with the resulting necrotic volume.

Among imaging modalities, MR possesses the unique benefit of having multiple measurable parameters that present temperature dependence, albeit of varying degree. The equilibrium magnetization M_0 is a function of temperature, cf. , but the effect is weak. The diffusion constant D has an exponential relationship with temperature, $D \propto \exp(-E_a/k_B T)$, where E_a is the apparent activation energy [68]. However, diffusion sensitive imaging is problematic because it requires long imaging times and is very sensitive to motion. The longitudinal relaxation time constant, T_1 , is affected by temperature through the changes in the rotational correlation time, τ_c , of the molecules. Temperature increase shortens τ_c as the molecules tumble more vigorously, which, at clinical field strengths, results in increased T_1 [10]. The molecular motion depends strongly on the molecule structure and the surrounding molecules; hence the change in T_1 is tissue dependant. Also the Larmor frequency exhibits temperature dependence: the chemical shift, that is, the magnetic screening caused by electron clouds in the proton surroundings, is affected by temperature. In water, increasing the temperature decreases hydrogen bonding, which distorts the electronic screening of the protons. This results in an increased screening effect and a decrease in the Larmor frequency. Because of the high water content in tissues, the effect is largely tissue independent and of the order of -0.01 ppm/°C in magnitude [69].

Larmor frequency and T_1 dependencies can be utilized in deducing tissue temperature in practice. As for the temperature measurement methods, their availability for interventional work depends on the scanner type used. With high field scanners, the temperature dependence of the Larmor frequency of protons is practical, whereas with the low field scanners T_1 dependency is more amenable [65]. There are several reasons for favouring frequency shift over T_1 dependency in high field systems: the small changes in the frequency are directly proportional to \mathbf{B}_0 ; the superconducting magnet of a high field scanner shields well against external, slowly varying magnet fields; and the \mathbf{B}_0 drift is less than that present in low field

electromagnets [70]. In both methods, the target volume is typically imaged before inducing the temperature changes. Subsequent fast imaging during the heating provides data that can be compared to the initial reference. In the T_1 -based method, the initial T_1 values are needed. Because of the difficulties in measuring small frequency shifts directly, the frequency changes are often measured as phase images, so an initial reference is also needed for the frequency dependent method.

2 Methods and Results

The methods described in this thesis were developed using a 0.23 T open configuration magnet (Panorama 0.23 T, Philips Medical Systems, Best, The Netherlands). However, they should be equally applicable on other low-field magnets of similar configuration.

2.1 Overhauser Enhanced Instrument Localization (I)

With low field scanners, the relatively low SNR prevents fast image acquisition and passive instrument tracking as very small features, such as those of a catheter, become hard to discern. Improving the contrast by flushing a catheter with a contrast agent bolus is only of limited help. In this work, a method utilising Overhauser enhancement *ex vivo* is presented that momentarily boosts the net magnetization of liquid that is then injected through the structure to be highlighted. When a target containing the structure is imaged, the enhanced liquid stands out against surrounding tissue where the signal level is lower, and the instrument can be localized.

To be practical, the paramagnetic agent used in enhancement should be easy to saturate, that is, have a narrow linewidth. It should be water-soluble, stable and non-toxic in diagnostic doses. An experimental trityl agent (NC100135, Amersham Health AB, Sweden) filled these requirements and was used in the experiments [71–73].

Overhauser enhancing requires irradiation of electron spins, which is technically challenging *in vivo* as the needed Larmor frequency is 658 times that of the protons. Here the enhancement was created *ex vivo*, with a separate resonator, so that the electronics could be made simple and power requirements modest. The resonator was supplied with propulsion mechanics to quickly (< 200 ms) deliver the enhanced 0.6 ml of 5 mM/l isotonic trityl solution into the target via 0.5 m of plastic tubing. The triggering signal from the mechanics was also connected to the scanner electronics, allowing a precise delay between the triggering event and image acquisition. The achievable enhancement was measured by injecting a bolus into the tube, and, after 0.5 s delay to reduce motion and flow artefacts, projection-imaging the tube with a single-shot fast-spin-echo (FSE) sequence (repetition time divided by echo time, TR/TE, set to

$\infty/219$ ms). The signal was compared with an unirradiated sample juxtaposed with the tube. An enhancement in excess of 10 was calculated and the concept demonstrated by acquiring projection images from a rat overlaid with the plastic tube.

2.2 ESR Probe for Instrument Tracking (II)

Many of the instrument-tracking systems rely on the assumption that the instrument to be tracked is rigid and position data can be extrapolated. However, with instruments like thin needles, this assumption is no longer valid and needle bending can result in a position error of several millimetres. One way to combat the error is to integrate a position-tracking element to the tip of the mandril. The small dimensions of thin needles make this exceedingly difficult with conventional means. In this work, a method is presented, where a sub-millimetre ESR sample is used for locating the needle tip.

The signal from electrons is significantly stronger than that of protons, as the gyromagnetic ratio, and hence the frequency, is higher. An ESR sample can therefore be very much smaller than the corresponding proton sample and still maintain the same SNR. The high Larmor frequency of the ESR sample requires somewhat complex receiving electronics, as microwave techniques must be adapted. In the article II, instead of receiving FIDs directly from the sample, a continuous wave method was used: A small sample of N-methylpyridinium (TCNQ, Amersham Health AB, Sweden), with approximate dimensions of $0.5 \times 0.5 \times 0.5$ mm, was glued with Epoxy into a small loop formed by the centre wire and the sheath at the terminating end of a coaxial cable resonator. It was irradiated at the resonant frequency of 6.45 GHz and the reflected power measured in presence of a low intermediate frequency (80 kHz) modulating magnetic field. The modulation was arranged with a separate coil. The change in susceptibility of the sample at resonance manifests in reduced power being reflected, so that after demodulation, the signal could be used as an input to a voltage controlled oscillator, hence locking the electronics to follow the resonant frequency of the sample. The signal after demodulation could also be used as an output, as it was directly related to the frequency in question. Sampling and averaging for 8 ms yielded values where the uncertainty was approximately $50 \text{ nT}_{\text{rms}}$.

For testing, the coaxial resonator was inserted into a 14 G biopsy sheath (Somatex GmbH, Germany) and a simple encoding gradient pulse scheme programmed to provide means for calculating position information. Needed gradients were modest, $250 \mu\text{T}/\text{m}$. To get quantitative data about the accuracy, 24 evenly spaced position data samples within a 300 mm isocentric sphere were measured with the ESR probe. The values were compared with the corresponding values measured from MR images of fiducial markers attached to the tip of the biopsy sheath. The error remained within ± 2 mm inside the sphere and was mainly influenced by the inaccuracies in determining the positions of MR visible fiducials.

Quasi real time tracking was demonstrated with a kiwi fruit: the needle was inserted into the fruit and position information displayed as an overlay on periodically updated images that showed the progress of the sheath as an artefact. The probe determined the centre positions of images, but as only translation information was available, the image planes were fixed. After

tracking the probe, the fruit was sectioned and photographed. The tracked path was overlaid on the photograph to visualize the close match with the physical path.

2.3 Optical Tracking (III–V)

In order to be able to better utilize the potential of optical tracking systems for MR guidance, close integration with the scanner is needed [74]: in addition to displaying the position data as an overlay or calculating multiplanar reconstruction images with it, the tracked instrument can also be used to set the position and orientation of intraoperative slice sets in an interactive manner. Periodically updated image sets help to reduce the risk of misaligning the instrument in a case of tissue deformations or organ movement, and provide confirmatory information about the instrument positions through the produced instrument artefact.

2.3.1 System Description

In this work, an optical tracking system was integrated with a scanner by modifying the user interface and scan-control software, and by altering an industrial tracking system to fulfil the requirements imposed on a medical device.

2.3.1.1 Hardware

The optical tracking system consisted of a commercial infrared camera with passive marker tracking capabilities (Polaris, Northern Digital Inc., Canada). The camera was attached to an adjustable and movable stand and linked to the controlling console with an armoured cable. Four magnet reference frames were fixed to the façade of the scanner to provide means to transform the coordinate system of the camera to that of the scanner. Each of the reference frames had four passive markers in a unique geometrical configuration and the camera was programmed to recognize each pattern. This way the camera could be moved around the scanner while maintaining a line-of-sight to at least one of the frames. The instrument trackers were similar to the reference frames: they consisted of three or four markers and mechanics for attaching them to instruments of different sizes. Because of the sterility requirements, only autoclavable materials such as Ultem[®] (General Electric Plastics, Massachusetts) and titanium were used in trackers.

In-room control electronics consisted of a 36" large screen display and a control pedestal with a mouse and a keyboard. In a typical use, the operator used the control pedestal under the instructions of the operating doctor, both of them having a line-of-sight to the display.

To augment system calibration, a special autocalibration phantom was constructed. It consisted of four paraffin oil-filled spheres placed in a slightly malformed tetrahedron. The malformation served to define a uniquely determinable rotation matrix for the phantom. That is, the known locations of the individual spheres in a physical coordinate space determined unambiguously the transformation matrix of the phantom in the said space. The phantom also had four passive markers for optical tracking and a titanium block with a small dimple for needle length determination. See Figure 6.

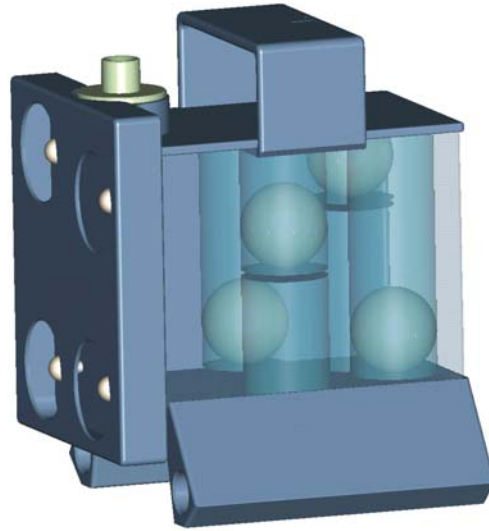


Figure 6. Autocalibration phantom. The phantom is made out of polyvinylchloride (PVC) and contains four oil-filled spheres. The sides are here shown as transparent for presentational clarity.

2.3.1.2 User Interface

The user interface had two main tasks. It had to provide simple and easily repeatable procedures for calibrating and verifying the operation of the optical system, and means for instrument visualization and intraoperative control of the scanner.

2.3.1.2.1 Calibration

The user interface provided means to calibrate the magnet reference frames automatically: the autocalibration phantom could be projection-imaged in three orthogonal planes and the oil-filled sphere locations calculated from the resulting images. With the sphere locations, the position and rotation information of the phantom could be expressed in magnet coordinates. The sphere locations could also be used in verification, as the relative physical positions of the spheres were known a priori. If the camera was moved to a position where it had a line-of-sight to both the phantom and one of the magnet reference frames, a transformation matrix could be calculated to express the phantom position in magnet reference frame coordinates and hence the link between magnet and reference frame coordinate systems found.

The instrument length, that is, the length from the origin of the attached instrument tracker to the tip of the instrument, could also be determined using the autocalibration phantom. This procedure is needed, because the needle-like instruments rarely are of a fixed length. In a calibration procedure, the tip of the instrument was placed into the dimple, the position of which was well defined on the phantom, and, providing the camera had a line-of-sight to both the phantom and the instrument, the length of the instrument was expressed in the coordinate system of the instrument tracker, yielding the needed offsets. See Figure 7.

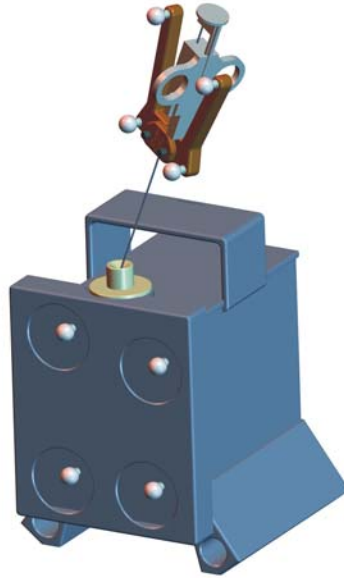


Figure 7. Calibration of the instrument length. The tip of the instrument is placed into the dimple on the autocalibration phantom, the user interface activated for a length calibration, and the tip held in place for two seconds while the relative positions of the instrument and the phantom are being repeatedly calculated to rule out spurious readings.

2.3.1.2.2 *Intraoperative Use*

A simple but intuitive method to give feedback on the instrument position is to use projected overlays of the instrument on the already acquired images. Using colour coding, the rudimentary depth information could be encoded into projected graphics, giving the user a sense whether the display object is above, in, or below a slice. Defining a target point on the image set allowed the use of aiming tools. See Figure 8. To be able to provide updated images in a fluoroscopic manner, the image acquisition was streamlined to consist only of the selection of a sequence type and imaging plane from pregenerated lists. The instrument tip and an optional push-depth offset along the instrument axis dictated the position of the centre slice to be acquired.

Another way of visualising the instrument was to use modest-size image sets and multiplanar reconstruction, where the instrument dictated the position and orientation of the reconstructed slice, see Figure 9.

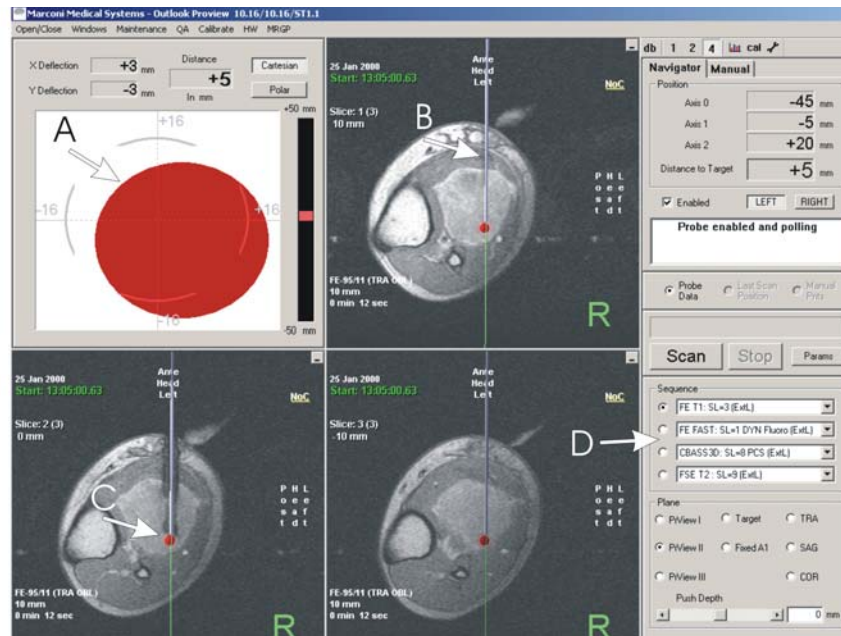


Figure 8. Intraoperative User Interface. A) A “bull’s-eye” aiming tool for aligning and guiding the instrument towards the target point. B) A projection of the needle above a slice. C) The red target point. D) Sequence shortcuts for quickly changing the sequence type during a procedure.

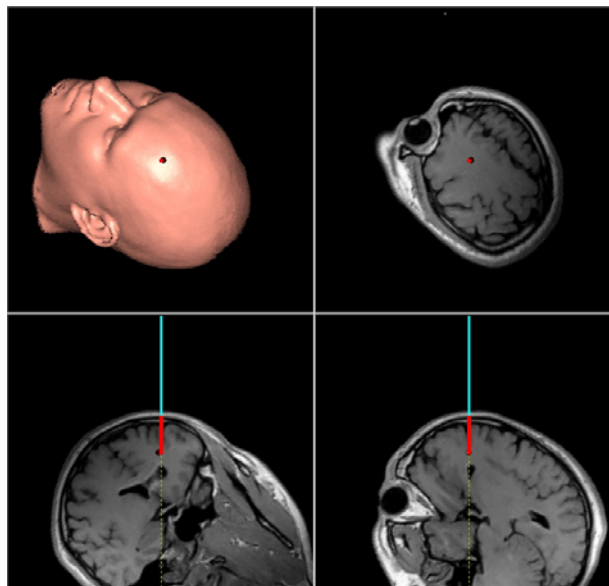


Figure 9. Multiplanar reconstruction. The upper left corner shows the surface rendered image set of a head, pointed at by an optically tracked instrument; the three remaining views display multiplanar reconstructed slices from the head. The slice orientations are orthogonal to each other and are derived from the instrument orientation.

2.3.2 Clinical Applications

The integrated optical tracking system was tested with applications where accuracy, ergonomics and intraoperative capabilities were required. The first two applications, nerve root infiltration and bone biopsy, could be performed with the intraoperative system. Because of the different nature of the third, a neurosurgical application, the system was augmented with task specific hardware and software.

2.3.2.1 Nerve Root Infiltration

In article III, the accuracy of the optical tracking system for the infiltration of the first sacral root was evaluated. The optical tracking system was used to align the needle towards the neural foramen using intraoperatively acquired images of different image planes. The needle was inserted and en-route acquired images used to confirm that the needle was correctly aligned and not bending. Instead of special contrast agents, the contrast, provided by injecting saline solution and imaging with a 128-echo single-shot FSE (TR/TE ∞ /274 ms, five 7 mm slices, acquired in 9 s), was sufficient for highlighting the nerve root sheath, thus confirming the correct final positioning of the instrument and allowing the injection of therapeutic agent.

Thirty-five infiltrations were performed on 34 patients with a success rate of 97% in positioning the needle into the nerve root foramen.

2.3.2.2 Bone Biopsies

In article IV, the optical tracking system was evaluated for guiding a bone biopsy set and acquiring images en-route. The biopsy set was MR-compatible and designed for optical navigation (BoneBiopsy, Daum GmbH, Germany) with a special adaptor piece. Biopsies were taken from five different anatomical regions: two from spine, one from sacral bone, one from femoral head and one from femoral diaphysis. The tracking system helped to determine the puncture route and the lesion could be approached more freely than with CT. The percutaneous procedures were performed in less than 40 minutes. All biopsies were successfully completed, without complications.

2.3.2.3 Patient Tracking

Limiting guidance of neurosurgical instruments to staged procedures (i.e. to procedures where the guiding and treatment is performed outside the scanner) degrades the usefulness of optical instrument tracking: The opening of the skull to access the surgical site may cause deformations of the brain. If only preoperative images were to be used, as is the case with stand-alone tracking systems, position errors larger than 10 mm could occur [75, 76]. However, many of the neurosurgical procedures require either the use of instruments that are not MR-compatible, or simply need too much space to be operated inside the scanner, effectively ruling out the intraoperative approach. In literature, methods, where the patient is transferred from operating room to the scanner in order to obtain intraoperative images, have been presented [77]. In addition to the safe transfer being difficult to arrange, this also means that possible optical tracking systems must be manually recalibrated after every transfer. In article V, a method to overcome the latter weakness is discussed.

In a neurosurgical operation, the head of the patient must be fixed. This is typically arranged with a head frame that is firmly fixed to the skull of the patient with screws. Here the frame was used as a mounting point for an additional optical reference frame, a ‘patient tracker’. Every time the patient was brought into the scanner, the patient tracker was recalibrated: when the camera had line-of-sight to both the patient tracker and one of the magnet trackers, the calibration data of the magnet tracker could be automatically applied to the patient tracker. When the patient was wheeled out of the magnet, the calibration data for the patient tracker and the acquired image set was still valid, presupposing the patient’s head had not moved with respect to the head frame—a safe assumption in this case. Because of the shutdown-capabilities of the magnet used in the experiments, the patient could be operated just outside the pole-pieces of the magnet. Were more images needed to rule out position errors due to tissue movement and deformations, or to check for the completeness of a resection, the magnet could be turned on in less than 10 minutes and patient rescanned.

The concept was demonstrated with two patient cases. Using updated images and the patient tracker, remaining tumour residuals could be pinpointed and anatomical structures located with clinically useful accuracy. The applicability to soft tissue biopsies was discussed [78, 79].

2.4 MR Thermometry of Liver Tissue (VI)

In the previous chapters, the emphasis has been on the instrument guidance. Article VI concerns the subsequent therapeutic step; in this case a liver tumour ablation. Means for predicting the necrotic volume through progressing temperature front were sought with a T_1 -based method for the temperature measurement of liver tissue.

The temperature sensitive parameters used were the equilibrium magnetization M_0 (approximately $-0.3\%/^{\circ}\text{C}$) and T_1 ($\sim 1\%/^{\circ}\text{C}$) [80]. The very small effect the temperature has on the Larmor frequency at 0.23 T was neglected. Because of sequence dependent T_1 behaviour and inherent SNR, different sequences were compared for the task using pig liver tissue samples. Spin echo, gradient echo and completely balanced SSFP sequences of clinically meaningful acquisition times were optimized to provide images with maximally temperature sensitive image intensity. The optimization parameters were TR for the spin echo sequence, and flip angles for the other two sequences. The signals from the optimized sequences were simulated for the liver tissue samples as a function of temperature. The simulations indicated that the inaccuracy in the temperature measured by the SSFP sequence was 50% of that of the spin echo sequence and 80% of that of the gradient echo sequence.

The temperature behaviour of the SSFP sequence was also determined experimentally. Extracted pig liver samples were heated with a hot water bath. The samples were scanned at 37°C (the reference temperature) and at elevated temperatures. Thermocouples embedded into the samples were used as a gold standard in determining the temperature, that is, the temperature values calculated from the image sets were compared against the values from the thermocouples. The optimization of the SSFP sequence was checked by measuring the noise in temperature measurements as a function of the flip angle at two different temperatures of 45°C and 55°C . The temperature inaccuracy of the optimized SSFP sequence was measured between 37°C and 60°C . The optimized flip angle was in agreement with the simulation

results: $63 \pm 8^{\circ}\text{C}$ versus the simulated 63°C . The temperature inaccuracy, 1.6°C , was twice the estimated value based on the simulation results.

3 Discussion

In article I, the ex vivo Overhauser enhancement and improved visibility of a catheter-like structure was successfully demonstrated. An enhancement factor of 10 was achieved, which corresponds to a proton signal at the field strength of 2.3 T, proving that a substantial signal gain is possible through the use of ex vivo-enhanced liquid. The method seems promising, considering that due to the oxygenation of the sample in the test set-up, a factor of two should be readily available with more careful control of oxygen concentration in enhancing liquid.

In article II, a miniaturized ESR Probe was designed into the tip of a needle-like structure. The construction allowed the probe to be inserted into a 14 G biopsy needle sheath. The probe was able to track the tip of the sheath at the rate of 10 samples per second with accuracy better than ± 2 mm, within a homogeneous sphere of 300 mm. The sampling rate is sufficient for quasi real time operation, especially when noting that typical bitmap refresh rates on the user interface displays are of the same order. The accuracy within the volume of interest is better than that of an optical tracking system: In addition to the insensitivity to the needle bending, also some of the image distortions, namely those introduced by non-linear gradients, are compensated. The tip tracking was successfully demonstrated with a kiwi fruit. Together with article I, these two methods illustrate how electron spin resonance can be used to boost the signal levels to achieve miniaturization needed for interventional tools. It should be noted that direct electron spin resonance signal is particularly well suited for miniaturization of field sensors: the fact that solid samples can be used makes the construction of the container for the sample simpler than is the case with liquids [81], whereas proton signals from solid samples can hardly be used at all: In the transition from a liquid to a solid, T_2 of proton spin system typically becomes exceedingly short [12, 82], and dipole-dipole couplings complicate the resonance spectra, together making position encoding with gradients almost impossible, not to mention much smaller SNR. It is relatively straightforward to protect a tiny ESR sample from tissue contact, which is a requirement for in vivo human experiments.

In article III, a customized optical tracking system and an MR scanner were used in deep neural tissue injections. The needle was placed, using the guidance system, 35 times into first sacral root foramina, with a success rate of 97%. No complications occurred. Based on the results, the combined use of the optical tracking system and 0.23 T magnet was considered

accurate, fast and suitable for the first sacral root infiltration. The conventional guiding methods in nerve root infiltrations have been fluoroscopy and CT. However, these methods require the use of contrast agents, cause harmful ionising radiation, and, in the case of fluoroscopy, leave room for improvement what comes to the depth resolution. Using the new method, the risks of ionising radiation from CT or fluoroscopy guided procedures could be eliminated, as well as the use of special contrast agents.

In article IV, the guiding system of article III was utilized in bone biopsies. Five biopsies from different anatomical areas were successfully obtained and the samples allowed for a pathologic diagnosis. The percutaneous procedures could be performed in less than 40 minutes. The method was deemed feasible, and had the benefits of superior bone and bone marrow lesion contrast [83] and lack of ionising radiation as compared to the CT or fluoroscopy guided procedures. Articles III and IV demonstrate the practical feasibility of the concept where an optical tracking system is integrated with an open configuration magnet, equipped with automated registration tools, reference frames and integrated guiding software so as to provide increased speed, accuracy and ergonomomy.

In article V, the optical navigator system was equipped with an additional patient tracking reference frame. The frame and the associated software provided the scanner with capabilities for on-site neuronavigation that could be combined with confirmatory intraoperative scanning. The concept was demonstrated with two patient cases. The patient tracker was used for pinpointing anatomical structures and helped to localize tumour remnants. The accuracy was improved, because images could be acquired after the dura was opened and tumour resected, that is, after the brain shift. The method made the procedures also faster and more ergonomic as there was no need for manual recalibration of the optical tracking system after the patient was removed from the magnet. Perhaps most importantly, the automated registration of image and tracking system coordinate spaces decreased the risk of human error: In methods where fiducials are manually pointed and identified on images, the chances for a mishap are real, especially when the registration procedure must be performed repeatedly. In the already complex operating environment associated with neurosurgery, and considering the possibly fatal consequences of large position errors, the accuracy, robustness and ergonomomy of the presented method should prove useful.

In article VI, a set of imaging sequences was discussed for temperature sensitive imaging of liver tissue at 0.23 T. Because of the low magnetic field strength, diffusion and proton frequency shift based methods were excluded, and the study concentrated on T_1 and M_0 temperature dependencies. Spin echo, gradient echo and completely balanced SSFP sequences were optimized for maximal temperature sensitivity and the optimized sequences compared using simulations. Based on the simulation results, the SSFP sequence was more accurate than the other two. The optimization data and temperature sensitivity of the SSFP sequence were further validated with in vitro measurements. The small heterogeneous sample and edge artefacts from the containing test tube were probable causes for the discovered discrepancy (a factor of two) between the simulated and measured results. It is inevitable that factors such as motion artefacts and perfusion in human subjects will degrade the accuracy in delineating the tissue destruction. But, considering the simulated and measured temperature inaccuracies, and the steep temperature gradients typically present in ablations, the SSFP sequence seems still to be a viable sequence type for a T_1 -based temperature monitoring at 0.23 T.

Methods used in interventional MRI are in the transition period to become a part of routine MRI. Because of the volatile state of the field, it is possible to adapt new approaches for performing procedures with relatively little resistance to change. This thesis illustrates methods and technology for facilitating some of the common interventional procedures on low field open configuration magnets, and demonstrates that real gain can be acquired from the use of the said methods.

4 Conclusions

This thesis addressed problems related to accurate localization of minimally invasive surgical tools and low field temperature monitoring of liver tissue.

1. Novel localization and guiding methods were presented:

- a) For a catheter localization, a method utilising ex vivo Overhauser enhancement of a catheter like structure for boosting the signal to noise ratio was demonstrated. Significant enhancement, that is, a factor of 10, was measured.
- b) A device for biopsy needle tip tracking was developed and its use demonstrated. The position of the tip was tracked with a signal from a miniaturized electron spin resonance sample and gradient pulses. The level of accuracy and acquisition speed was sufficient for interventional work, the accuracy being better than that of a typical optical tracking system and the speed comparable

2. New methods and indications of use were developed for an optical tracking system:

- a) An optical guidance system was integrated with an open-configuration magnet and used intraoperatively, proving clinically feasible, fast, ergonomic and accurate in sacral root infiltrations and bone-biopsies.
- b) The guidance system was further customized for staged neurosurgical procedures, and the ergonomics and versatility of the system demonstrated with patient cases.

3. Means for qualitative low field MR temperature measurement of liver tissue was examined. Based on the in vitro experiments, an optimized completely balanced steady-state sequence seemed to be a sufficiently accurate temperature measurement sequence for a low field scanner, with potential for limiting the damage to healthy liver tissue and helping to determine the complete destruction of the tumour.

All combined, the studies demonstrate the usefulness and versatility of magnetic resonance imaging for interventional work.

5 References

- 1 Damadian R, Minkoff L, Goldsmith M, Stanford M., Koutcher J. Field Focusing Nuclear Magnetic Resonance (FONAR): Visualization of a Tumor in a Live Animal. *Science* 194:1430 (1976).
- 2 Ogawa S, Menon RS, Kim SG, Ugurbil K. On the Characteristics of Functional Magnetic Resonance Imaging of the Brain. *Annual Review of Biophysics and Biomolecular Structure*. 27:447–74 (1998).
- 3 Jolesz FA, Zientara GP. MRI-Guided Interventions. In: Edelman RR, Zlatkin MB, Hesselink JR, editors. *Clinical Magnetic Resonance Imaging* (2nd ed). W.B. Saunders Company, Philadelphia, PA: (1996).
- 4 Wallis F, Gilbert FJ. Magnetic resonance imaging in oncology: an overview. *Journal of the Royal College of Surgeons of Edinburgh* 44(2):117–125 (1999).
- 5 Shellock, FG, Kanal, E. *Magnetic Resonance; Bioeffects, Safety, and Patient Management* (2nd ed). Lippincott-Raven Press, Philadelphia PA (1996).
- 6 Kacher DF, Nabavi A, Kanan R, Koran SJ, Sela G, White CA, Bronskill MJ, Jolesz FA. Design and Implementation of Surgical Instruments, Devices, and Receiver Coils for Intraoperative MRI-Guided Neurosurgical and Neuroablative Procedures. *Automedica* 20:89–134 (2001).
- 7 Shellock FG. Metallic Surgical Instruments for Interventional MRI Procedures: Evaluation of MR Safety. *Journal of Magnetic Resonance Imaging* 13:152–157 (2001).
- 8 Jolesz FA, Blumenfeld SM. Interventional Use of Magnetic Resonance Imaging. *Magnetic Resonance Quarterly* 10:85–96 (1994).
- 9 Patel KC, Duerk JL, Zhang Q, Chung YC, Williams M, Kaczynski K, Wendt M, Lewin JS. Methods for Providing Probe Position and Temperature Information on MR Images During Interventional Procedures. *IEEE Transactions on Medical Imaging* 17(5):794–802 (1998).
- 10 Callaghan PT. *Principles of Nuclear Magnetic Resonance Microscopy*. Oxford University Press, Oxford (1995).
- 11 Brehm JJ, Mullin WJ. *Introduction to the Structure of Matter*. John Wiley & Sons, New York (1989).
- 12 Abragam A. *Principles of Nuclear Magnetism*. Oxford University Press, Oxford (1999).
- 13 Lauterbur PC. Image formation by induced local interactions: Examples employing nuclear magnetic resonance. *Nature* 242:190–191 (1973).
- 14 Ljunggren S. A Simple Graphical Representation of Fourier-Based Imaging Methods. *Journal of Magnetic Resonance* 54:338–343 (1983).
- 15 Liang Z-P, Lauterbur PC. *Principles of Magnetic Resonance Imaging*. IEEE Press, New York (2000).

-
- 16 Jeschke G. New Concepts in Solid-State Pulse Electron Spin Resonance. PhD Thesis, Swiss Federal Institute of Technology Zürich, Diss. ETH No. 11873 (1996).
 - 17 Ylihautala M, Ehnholm G, Vahala E, Jyrkinen L, Tervonen O. Instrument Localization in MRI Using Electron Spin Resonance. Proceedings of the 9th Annual Meeting of the International Society for Magnetic Resonance in Medicine, Glasgow:546 (2001).
 - 18 Duret D, Beranger M, Moussavi M, Turek P, Andre JJ. A new ultra low-field ESR spectrometer. Review of Scientific Instruments, American Institute of Physics 62(3):685–694 (1991).
 - 19 Nieminen J, Magneettikentän mittaaminen mikroaaltoresonaattorilla. Master's Thesis, Helsinki University of Technology (1993).
 - 20 Schweiger A. New trends in pulsed EPR methodology. In: Modern pulsed and continuous wave electron spin resonance, Kevan L, Bowman M (Eds.), Wiley, New York (1990).
 - 21 Slichter CP. Principles of Magnetic Resonance. 3rd ed. Springer-Verlag Berlin Heidelberg (1990).
 - 22 Lurie DJ, Hutchison JMS, Bell LH, Nicholson I, Bussell DM, Mallard JR. Field-Cycled Proton-Electron Double-Resonance Imaging of Free Radicals in Large Aqueous Samples. Journal of Magnetic Resonance 84:431–437 (1989).
 - 23 Lurie DJ, Nicholson I. Proton-Electron Double-Resonance Imaging of Exogenous and Endogenous Free Radicals In-Vivo, In: Proceedings of International School of Physics Enrico Fermi, Course CXXIII, Nuclear Magnetic Double Resonance, Maraviglia B. (Ed.), North Holland, Amsterdam (1993).
 - 24 Joensuu RP, Sepponen RE, Lamminen AE, Savolainen SE, Standertskjöld-Nordenstam C-GM. High-Accuracy MR Tracking of Interventional Devices: the Overhauser Marker Enhancement (OMEN) Technique. Magnetic Resonance in Medicine 40:914–921 (1998).
 - 25 Watanabe E, Watanabe T, Manaka S, Mayanagi Y, Takakura K. Three dimensional digitizer (Neuronavigator): New Equipment of Computed Tomography-Guided Stereotaxic Surgery. Surgical Neurology 27:543–547, 1987.
 - 26 Sipos EP, Tebo SA, Zinreich SJ, Long DM, Brem H. In Vivo Accuracy Testing and Clinical Experience with the ISG Viewing Wand. Neurosurgery 39:194–202 (1996).
 - 27 Barnett GH, Kormos DW, Steiner CP, Weisenberger J. Intraoperative Localization Using an Armless, Frameless Stereotactic Wand. Journal of Neurosurgery, 78:510–514. 1993.
 - 28 Grimson E, Leventon M, Ettinger G, Chabrierie A, Ozlen F, Nakajima S, Atsumi H, Kikinis R, Black P. Clinical Experience with High Precision Image-Guided Neurosurgery System. Lecture Notes in Computer Science 1496:63–73 (1998).
 - 29 Ganslandt O, Steinmeier R, Kober H, Vieth J, Kassubek J, Romstöck J, Strauss C, Fahlbusch R. Magnetic Source Imaging Combined with Image-Guided Frameless Stereotaxy: A New Method in Surgery around the Motor Strip. Neurosurgery 41:621–627 (1997).
 - 30 Leksell L. A stereotaxic apparatus for intracerebral surgery. Acta Chirurgica Scandinavica 99:229–233 (1949).

-
- 31 Leksell LA. Stereotaxic Method and Radiosurgery of the Brain. *Acta Chirurgica Scandinavica* 102:316–319 (1951).
 - 32 Kamiryo T, Laws ER Jr. Stereotactic frame-based error in magnetic-resonance-guided stereotactic procedures: a method for measurement of error and standardization of technique. *Stereotactic and Functional Neurosurgery* 67(3–4):198–209,1996-97.
 - 33 Silverman SG, Collick BD, Figueira MR, Khorasani R, Adams DF, Newman RW, Topulos GP, Jolesz FA. Interactive MR-guided Biopsy in an Open-Configuration MR Imaging System. *Radiology* 197:175–181 (1995).
 - 34 Dumoulin CL, Souza SP, Darrow RD. Real-Time Position Monitoring of Invasive Devices Using Magnetic Resonance. *Magnetic Resonance in Medicine* 29:411–415 (1993).
 - 35 Leung DA, Debatin JF, Wildermuth S, Heske N, Dumoulin CL, Darrow RD, Hauser M, Davis CP, von Schulthess GK. Real-Time Biplanar Needle Tracking for Interventional MR Imaging Procedures. *Radiology* 197:485–488 (1995).
 - 36 Burl M, Coutts GA, Young IR. Tuned Fiducial Markers to Identify Body Locations with Minimal Perturbation of Tissue Magnetization. *Magnetic Resonance in Medicine* 36:491–493 (1996).
 - 37 Coutts GA, Gilderdale DJ, Chui M, Kasuboski L, DeSouza NM. Integrated and Interactive Position Tracking and Imaging of Interventional Tools and Internal Devices Using Small Fiducial Receiver Coils. *Magnetic Resonance in Medicine* 40:908–913 (1998).
 - 38 Glowinski A, Adam G, Bücker A, Neuerburg J, van Vaals JJ, Günther RW. Catheter Visualization for Interventional MR by Actively Controlled Locally Induced Field Inhomogeneities. *Proceedings of the 4th Annual Meeting of International Society of Magnetic Resonance in Medicine*, Vol 1:51 (1996).
 - 39 Lewin JS, Duerk JL, Jain VR, Petersilge CA, Chao CP, Haaga JR. Needle Localization in MR-Guided Biopsy and Aspiration: Effects of Field Strength, Sequence Design, and Magnetic Field Orientation. *American Journal of Roentgenology* 166(6):1337–1345 (1996).
 - 40 Reichenbach JR, Wurdinger S, Pfeiderer SOR, Kaiser WA. Comparison of Artifacts Produced From Carbon Fiber and Titanium Alloy Needles at 1.5 T MR Imaging. *Journal of Magnetic Resonance Imaging* 11:69–74 (2000).
 - 41 Brenner RJ, Shellock FG, Rothman BJ, Giuliano A. Technical note: magnetic resonance imaging-guided pre-operative breast localization using “freehand technique.” *The British Journal of Radiology* 68:1095–1098 (1995).
 - 42 Rubin DL, Ratner AV, Young SW. Magnetic susceptibility effects and their application in the development of new ferromagnetic catheters for magnetic resonance imaging. *Investigative Radiology* 25:1325–1332 (1990).
 - 43 Bakker CJ, Hoogeveen RM, Weber J, van Vaals JJ, Viergever MA, Mali WP. Visualization of dedicated catheters using fast scanning techniques with potential for MR-guided vascular interventions. *Magnetic Resonance in Medicine* 36:816–820 (1996).
 - 44 Daniel BL, Birdwell RL, Ikeda DM, Jeffrey SS, Black JW, Block WF, Sawyer-Glover AM, Glover GH, Herfkens RJ. Breast lesion localization: a freehand, interactive MR imaging-guided technique. *Radiology* 207:455–463 (1998).

-
- 45 Unal O, Korosec FR, Frayne R, Strother CM, Mistretta CA. A Rapid 2D Time-Resolved Variable-Rate k-space Sampling MR Technique for Passive Catheter Tracking During Endovascular Procedures. *Magnetic Resonance in Medicine* 40:356–362 (1998).
 - 46 Brown RA, Roberts TS, Osborne AG. Stereotactic frame and computer software for CT-directed neurosurgical localization. *Investigative Radiology* 15:308–312 (1980).
 - 47 Leksell L, Jerenberg B. Stereotaxis and tomography: a technical note. *Acta Neurochirurgica* 52:1–7 (1980).
 - 48 Sandeman DR, Patel N, Chandler C, Nelson RJ, Coakham HB, Griffith HB. Advances in image-directed neurosurgery: preliminary experience with the ISG viewing wand compared with the Leksell G frame. *The British Journal of Neurosurgery* 8:529–544 (1994).
 - 49 Pèria O, Chevalier L, François-Jaubert A, Caravel JP, Dalsogliò S, Lavallée S, Cinquin P. Using a 3D-position sensor for registration of SPECT and US images of the kidney. *Computer Vision, Virtual Reality and Robotics in Medicine, 1st International Conference CVRMed '95, Nice, France, April. 23–29 (1995).*
 - 50 Lee MH, Lufkin RB, Borges A, Lu DSK, Sinha S, Farahani K, Villabalanca P, Curran J, Hall T, Atkinson D, Kangaroo H. MR-Guided Procedures Using Contemporaneous Imaging Frameless Stereotaxis in an Open-Configuration System. *Journal of Computer Assisted Tomography* 22(6):998–1005 (1998).
 - 51 Dorward NL, Alberti O, Velani B, Gerritsen FA, Harkness WF, Kitchen ND, Thomas DG. Postimaging brain distortion: magnitude, correlates, and impact on neuronavigation. *Journal of Neurosurgery* 88:656–62 (1998).
 - 52 Black PMcL, Mortiarty T, Alexander E III, Stieg P, Woodard EJ, Gleason PL, Martin CH, Kikinis R, Schwartz RB, Jolesz FA. Development and Implementation of Intraoperative Magnetic Resonance Imaging and its Neurosurgical Applications. *Neurosurgery* 41:831–845 (1997).
 - 53 Schenck JF, Jolesz FA, Roemer PB, Cline HE, Lorensen WE, Kikinis R, Silverman SG, Hardy CJ, Barber WD, Lakaris ET, Dorri B, Newman RW, Holley CE, Collick BD, Dietz DP, Mack DC, Ainslee MD, Jaslolski PL, FigueiraMR, vom Lehn JC, Souza SP, Dumoulin CL, Darrow RD, Peters RL, Rohling KW, Watkins RD, Eisner DR, Blumenfeld SM, Vosburgh KG. Superconducting open-configuration MR imaging system for image-guided therapy. *Radiology* 195: 805–814 (1995).
 - 54 Lees WR, Gilliams AR, Smart SC, Kaczynski KR. A passive navigation device for interactive slice positioning in interventional MRI. *European Congress of Radiology '99, Viena, Austria:522 (1999).*
 - 55 Birkfellner W, Watzinger F, Wanschitz F, Ewers R, Bergmann H. Calibration of Tracking Systems in a Surgical Environment. *IEEE Transactions on Medical Imaging* 17(5):737–742 (1998).
 - 56 Rohling R, Munger P, Hollerbach JM, Peters T. Comparison of Relative Accuracy Between a Mechanical and an Optical Position Tracker for Image-Guided Neurosurgery. *Journal of Image Guided Surgery* 1:30–34 (1995).

-
- 57 Fitzpatrick JM, West JB. The Distribution of Target Registration Error in Rigid-Body Point-Based Registration. *IEEE Transactions on Medical Imaging* 20(9):917–927 (2001).
- 58 de Zwart JA, Salomir R, Vimeux F, Klaveness J, Moonen CTW. On the Feasibility Of Local Drug Delivery Using Thermo-Sensitive Liposomes and MR-Guided Focused Ultrasound. *Proceedings of the 8th Annual Meeting of the International Society of Magnetic Resonance in Medicine*, Denver:43 (2000).
- 59 Groenemeyer DHW, Schirp S, Gevargez A. Image-guided Percutaneous Thermal Ablation of Bone Tumors. *Academic Radiology* 9(4):467–477 (2002).
- 60 Schwarzmaier HJ, Kahn T. Magnetic resonance imaging of micro-wave induced tissue heating. *Magnetic Resonance in Medicine* 33:729–731 (1995).
- 61 Hyodoh H, Furuse M, Kawamoto C, Isoda N, Ido K, Saito K. Microwave Coagulation Therapy: Ex Vivo Comparison of MR Imaging and Histopathology. *Journal of Magnetic Resonance Imaging* 11:168–173 (2000).
- 62 Cline HE, Hynynen K, Hardy CJ, Watkins RD, Schenck JF, Jolesz FA. MR temperature mapping of focused ultrasound surgery. *Magnetic Resonance in Medicine* 31:628–636 (1994).
- 63 Sewell PE, Arriola RM, Robinette L, Cowan BD. Real-Time I-MR-Imaging-guided Cryoablation of Uterine Fibroids. *Journal of Vascular and Interventional Radiology* 12(7):891–893 (2001).
- 64 Il'Yasov KA, Bjørnerud A, Rogstad A, Wiggen UN, Henriksen I, Eissner B, Hennig J, Fossheim SL. Paramagnetic Liposomes as Thermosensitive Probes for MRI-Guided Thermal Ablation: Feasibility Study on the Perfused Porcine Kidney. *Proceedings of the 9th Annual Meeting of the International Society for Magnetic Resonance in Medicine*, Glasgow:324 (2001).
- 65 Quesson B, de Zwart JA, Moonen CTW. Magnetic Resonance Temperature Imaging for Guidance of Thermotherapy. *Journal of Magnetic Resonance Imaging* 12:525–533 (2000).
- 66 Lewin JS, Connell CF, Duerk JL, Chung Y-C, Clampitt ME, Spisak J, Gazelle GS, Haaga JR. Interactive MRI-Guided Radiofrequency Interstitial Thermal Ablation of Abdominal Tumors: Clinical Trial for Evaluation of Safety and Feasibility. *Journal of Magnetic Resonance Imaging* 8(1):40–47 (1998).
- 67 Vogl TJ, Mack MG, Straub R, Eichler K, Engelmann K, Zangos S, Voitazek D. MR Guided Laser-Induced Thermotherapy (LITT) of Malignant Liver and Soft Tissue Tumours. *Medical Laser Application* 16(2):91–102 (2001).
- 68 Schüring A, Auerbach SM, Fritzsche S, Haberlandt R. On Entropic Barriers for Diffusion in Zeolites: A Molecular Dynamics Study. *Journal of Chemical Physics* 116(24): 10890–10894 (2002).
- 69 Chung YC, Duerk LJ, Shankaranarayanan A, Hampke M, Merkle EM, Lewin JS. Temperature Measurement Using Echo-Shifted FLASH at Low Field for Interventional MRI. *Journal of Magnetic Resonance Imaging* 9:138–145 (1999).

-
- 70 Sinha S, Oshiro T, Sinha U, Lufkin R. Phase Imaging on a .2-T MR Scanner: Application to Temperature Monitoring During Ablation Procedures. *Journal of Magnetic Resonance Imaging* 7:918–928 (1997).
- 71 Konijnenburg H, Wistrand L-G, Trommel J, Mehlkopf AF. A promising new contrast agent for Overhauser imaging. *Magnetic Resonance Materials in Physics, Biology, and Medicine* 4(2nd supplement):72 (1996).
- 72 Ardenkjær-Larsen JH, Laursen I, Leunbach I, Ehnholm G, Wistrand L-G, Petersson JS, Golman K. EPR and DNP Properties of Certain Novel Single Electron Contrast Agents Intended for Oximetric Imaging. *Journal of Magnetic Resonance* 133:1–12 (1998).
- 73 Andersson S, Radner F, Rydbeck A, Servin R, Wistrand L-G. Free Radicals. US Patent 5530140 (1996).
- 74 Jyrkinen L, Ojala R, Haataja L, Blanco R, Klemola R, Silven O, Tervonen O. Managing the complexity of the user interface of a MRI guided surgery system. Proceedings of the 6th ERCIM “User Interfaces for All” Workshop, Florence (2000).
- 75 Hill DL, Maurer CRJ, Maciunas RJ, Barwise JA, Fitzpatrick JM, Wang MY. Measurement of intraoperative brain surface deformation under a craniotomy. *Neurosurgery* 43(3):514–528 (1998).
- 76 Fahlbusch R, Ganslandt O, Nimsky C. Intraoperative imaging with open magnetic resonance imaging and neuronavigation. *Child’s Nervous System: ChNS: official journal of the International Society for Pediatric Neurosurgery* 16:829–831 (2000).
- 77 Tronnier VM, Wirtz CR, Knauth M, Lenz G, Pastyr O, Bonsanto MM, Albert F, Kuth R, Staubert A, Schlegel W, Sartor K, Kunze S. Intraoperative Diagnostic and Interventional Magnetic Resonance Imaging in Neurosurgery. *Neurosurgery* 40(5):891–902 (1997).
- 78 Vahala E, Parkkola R, Ojala R, Vaara T, Ylihautala M, Ehnholm G. Registration of Optical Navigator in Staged Musculoskeletal Procedures. Proceedings of the 9th Annual Meeting of the International Society for Magnetic Resonance in Medicine, Glasgow:2183 (2001).
- 79 Vetter T, Oppelt A. Navigation as a Supplement for an Open MR System. *Minimally Invasive Therapy* Vol 9 Nr ¾, Aug 2000.
- 80 Germain D, Chevallier P, Laurent A, Savart M, Wassef M, Saint-Jalmes H. MR monitoring of laser-induced lesions of the liver in a low field open magnet: temperature mapping and lesion size prediction. *Journal of Magnetic Resonance Imaging* 13:42–49 (2001).
- 81 Joensuu RP, Sepponen RE, Lamminen AE, Standertskjöld-Nordenstam. A Shielded Overhauser Marker for MR Tracking of Interventional Devices. *Magnetic Resonance in Medicine* 43:139–145 (2000).
- 82 Ylihautala M. NMR of Small Solutes in Liquid Crystals and Molecular Sieves. PhD Thesis, University of Oulu. *Acta Universitatis Ouluensis* A330 (1999).
- 83 Parkkola RK, Mattila KT, Heikkilä JT, Ekfors TO, Kallajoki MA, Komu MES, Vaara TJ, Aro HT. Dynamic contrast-enhanced MR imaging and MR-guided bone biopsy on a 0.23 T open imager. *Skeletal Radiology* 30:620–624 (2001). DOI 10.1007/s002560100415.